Steady State Modeling and Performance Analysis of Static Slip Energy Recovery Controlled Slip Ring Induction Motor Drive

B. K. Singh and K. B. Naik

Abstract: The paper deals with steady state modeling of static slip energy recovery controlled slip ring induction motor drive. The dc equivalent circuit model of the drive is developed using power balance relationship. The steady state performance equations of the drive are derived using the model. The predicted performance characteristics of the drive are compared with the experimental investigation. The good degree of agreement of the computed results with experimental ones proves the validity of the developed model of the drive.

Key words: Energy, Induction motor, Recovery, Slip

I. INTRODUCTION

With the production of silicon diode and silicon controlled rectifier of adequately large ratings it becomes possible to replace all auxiliary machines of the traditional Scherbius drive by a three phase bridge rectifier and static inverter resulting in more compact static slip energy recovery (SER) controlled slip ring induction motor drive[1]. The static SER induction motor drive is popular among variable speed ac drives because of its inherent characteristics of higher efficiency, low converter cost and simple control circuit. It is being used in industrial applications such as, crane, hoist, pump and fan [2]. The speed control of the drive is achieved by regulating the rotor voltage through the firing angle of the phase commutated inverter [3]. When the firing angle is increased, high dc output voltage of the inverter prohibits the flow of rotor current, resulting low generation of torque, thereby, low speed of the drive. On the other hand if the firing angle is increased, small dc output voltage of the inverter permits the flow of higher rotor current, resulting high torque and high speed.

The modeling of static SER induction motor drive has been approached by large number of authors.

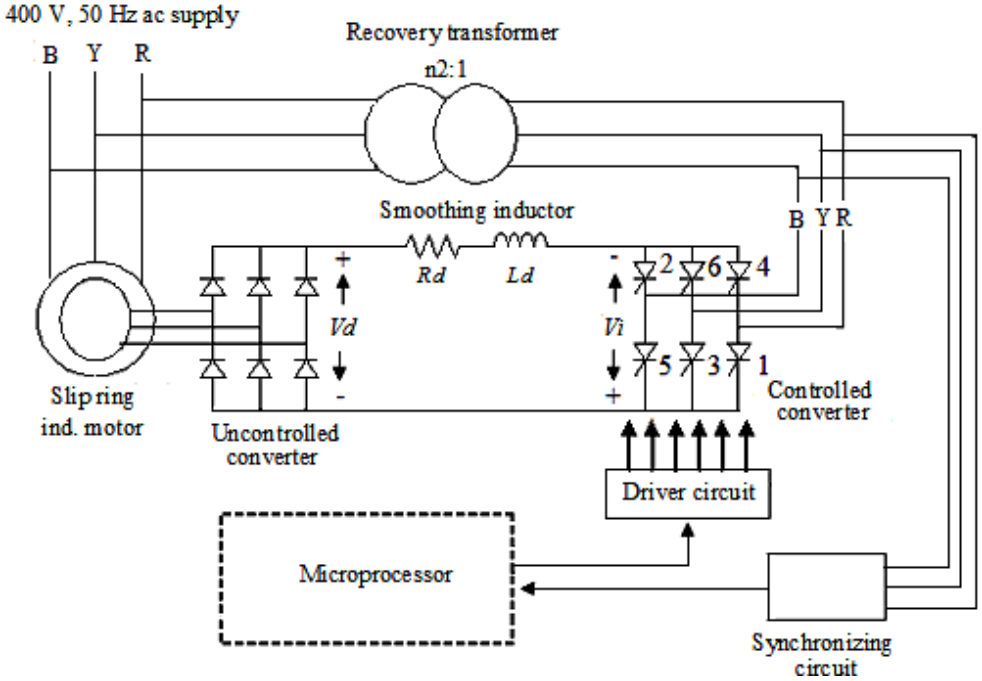

Fig. 1 Schematic block diagram of static SER controlled slip ring induction motor drive

Manuscript received on December 28, 2008.

B. K. Singh is with Electronics and Comm. Engg. Department, Kumaon Engineering College, Dwarahat, Almora, Uttarakhand, India: 2636553 (Phone No. 915966-244107; Fax: 915966-244114, e-mail: bksapkec@yahoo.com

K. B. Naik is with College of Engineering Science & Technology, Lucknow, U. P., India, e-mail: kbnaik@yahoo.com

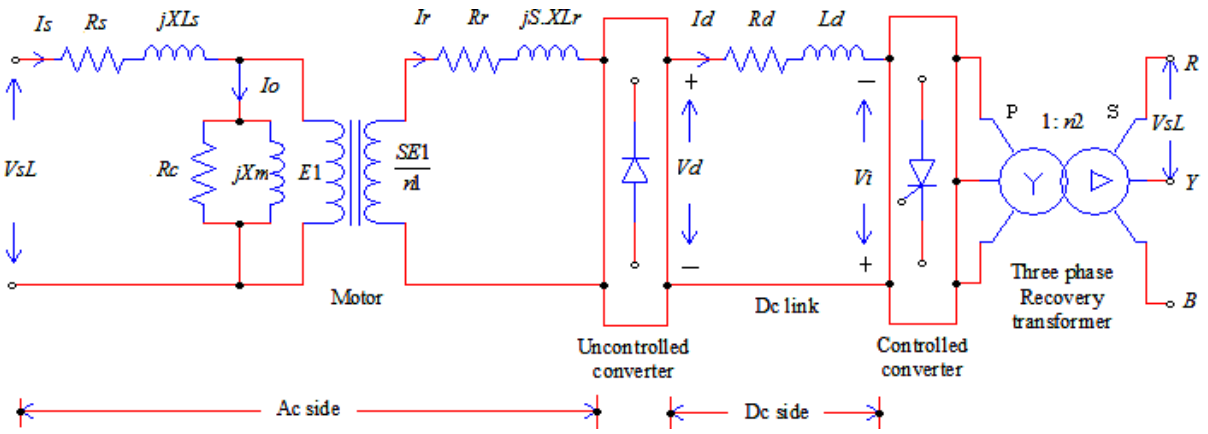

Fig. 2 Hybrid equivalent circuit of static SER controlled slip ring induction motor drive

Pavlov et al. developed a hybrid SER controlled slip ring induction motor drive [4] in which subsynchronous was one mode of operation. They included the motor leakage reactance in steady state analysis. Mittle et al. [5] presented the starting transients of static SER induction motor drive operating in subsynchronous range of speed using a set of non-linear differential equations developed using d-q model in synchronously rotating reference frame. The non-linear differential equations were simulated on a digital computer and solved using Runga-Kutta method. The effects of firing angle, load, system inertia and filter time constant on transient torques and speeds following a switching operation were investigated. Brown et al. [6] proposed a model which was hybrid between the traditional d-q and a-b-c models in which the rotor circuit was kept intact with transformation applied to the stator circuits only. Using the proposed model the steady state behavior of the drive was predicted. P. C. Krause [7] et al. corrected the assumptions of the model used in paper [5] and predicted the steady state performance of the drive operating in subsynchronous range of speed using synchronously rotating reference frame model. E. Akpinar and P. Pillay [8] developed a hybrid model of the drive in which actual rotor phase variables were retained and transformed the stator phase variables. The steady-state and transient performances of the drive were examined considering commutation overlap and harmonics of the rectifier and the inverter. The inclusion of effects of commutation overlap and harmonics added the complexity of the model. S. A. Papathanassiou and M. P. Papadopoulos [9] developed simplified 5th order d-q dynamic model utilizing the arbitrary reference frame and predicted the dynamic behavior of SER controlled slip ring induction motor drive.. The papers discussed above [4] – [9] used different forms of complex d-q model for the performance investigation of static SER controlled slip ring induction motor drive. Hence, there is a need to develop a simple model which may include the major effect of commutation overlap of the rectifier. The drive under investigation consists of a three phase slip ring induction motor, a three phase uncontrolled converter, a smoothing inductor, a three phase controlled converter and a three phase step up transformer. The schematic diagram of the drive is shown in Fig. 1. In the present work, the steady-state modeling and analysis of static SER controlled slip ring induction motor drive are presented. The steady-state performance characteristics of the drive are computed using developed dc equivalent circuit model. The predicted performance characteristics are verified with the experimental investigations.

II. DEVELOPMENT OF HYBRID EQUIVALENT CIRCUIT MODEL

The hybrid equivalent circuit of static SER controlled slip ring induction motor drive shown in Fig. 2 consists of per phase equivalent circuit of three phase induction motor, a three phase uncontrolled converter, dc link circuit consisting of smoothing inductor, a three phase controlled converter and a three phase recovery transformer. Applying the methodology discussed in paper [10] the dc equivalent circuit model is developed using hybrid equivalent circuit.

III. DEVELOPMENT OF DC EQUIVALENT CIRCUIT MODEL

For the development of dc equivalent circuit model, the following simplifying assumptions are made [11]. 1 The commutation distortion effect in the rotor current wave due to leakage inductance of the motor is ignored. 2. The dc link current *Id* is assumed to be ripple free as high value of inductor is connected in the dc link circuit. 3. The harmonics injected into the motor are considered to be fed from

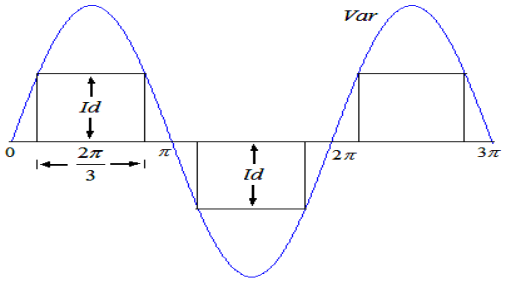

Fig. 3 Rotor phase voltage and phase current

the rotor by a current source. As harmonics in the rotor current cause only a small harmonics current to flow in the stator, the machine induced emf and hence, the flux is assumed to be sinusoidal and the torque is produced only by the fundamental component while harmonics produce only pulsating torque. 4. Thyristors and diodes are assumed to be ideal. 5. The recovery transformer is assumed to be ideal i.e. it is having no leakage, no loss and capability of exactly transforming a six step current wave from the controlled converter to the ac mains. 6. The commutation overlap effect in the controlled converter is neglected. 7. The effect of magnetizing current being very small is neglected

Based on these assumptions, a fundamental frequency per phase dc equivalent circuit model of the static SER controlled slip ring induction motor is developed. For the development of the model, all the parameters of primary side of the motor are transferred to the secondary side and then the transferred and secondary parameters are referred to the dc link side. The ac side resistances Rs' and Rr are translated to the dc side by balancing the power losses. As the dc link current is assumed ripple free, the rotor phase current is a six step wave shown in Fig. 3 and its magnitude is equal to the dc link current Id . The fundamental rotor phase current is in phase with the phase voltage. The rms value of rotor phase current is given as:

$$Ir = [\frac{1}{\pi}\int_{0}^{\frac{2.\pi}{3}} Id^2 .d(\omega t)]^{\frac{1}{2}} = \frac{\sqrt{2}}{\sqrt{3}} Id \quad (1)$$

The ac side resistances are translated to the dc side by balancing the power losses.

$$3.Ir^2[S.Rs' + Rr] = Id^2 \,\mathrm{Re} \quad (2)$$

Substituting equation (1) it yields

$$\mathrm{Re} = 2(S.Rs' + Rr) \quad (3)$$

Due to presence of stator and rotor leakage reactances $S.XLs'$ and $S.XLr$, the transfer of the current between diodes of the uncontrolled converter is no longer instantaneous. There is a period of overlap in which two phases carry current simultaneously. This causes a voltage drop V_R from the terminals of the rectifier bridge [11] which is given by

$$V_R = 3.S(XLs' + XLr)Id/\pi \quad (4)$$

This voltage drop is responsible for power loss in the rotor circuit and hence, considered as a fictitious reactance $3.S(XLs' + XLr)/\pi$ in the dc equivalent circuit. As the effect of magnetizing current is neglected, the drive is represented by the dc equivalent circuit as shown in Fig. 4, where all the parameters of the ac side of the hybrid equivalent circuit model are referred to the dc link side. The expressions of output dc voltages Vd and Vi of the uncontrolled and controlled converters respectively are given as:

$$Vd = \frac{3\sqrt{6}}{\pi}\frac{S.VsL}{n1} \quad (5)$$

$$Vi = \frac{3\sqrt{6}}{\pi}\frac{VsLCos\alpha}{n2} \quad (6)$$

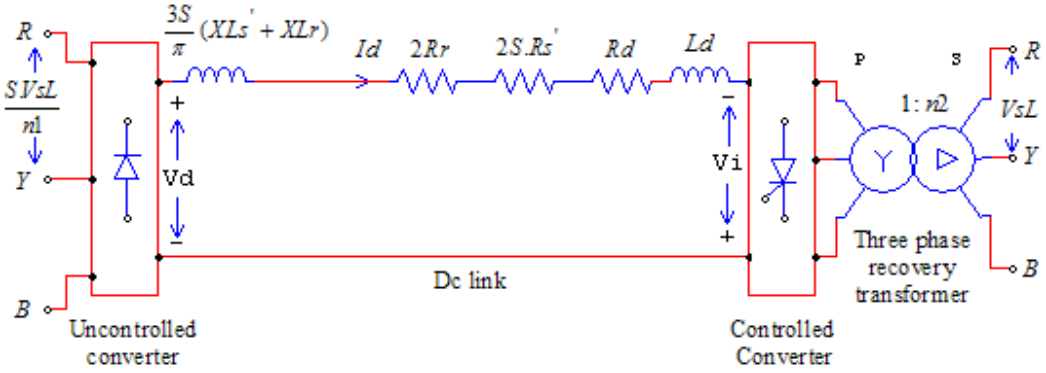

Fig. 4 Dc equivalent circuit of static SER controlled slip ring induction motor drive

Performance Equations: The inductance of the smoothing inductor is not considered in deriving the steady state performance equations, as its effect in steady state is zero. Since, $3.S(XLs' + XLr)/\pi$ represents commutation overlap and $2.S.Rs'$ the equivalent stator resistance, hence, parameters are not considered in determination of rotor copper loss. The copper loss of rotor is determined as follows:

$$\Pr cu = [Vd - \{\frac{3S}{\pi}(XLs' + XLr) + 2SRs'\}Id]Id \quad (7)$$

Further, the above equation is simplified as:

$$\Pr cu = Vd.Id - S.rs.Id^2 \quad (8)$$

where,

$$rs = \frac{3}{\pi}(XLs' + XLr) + 2.Rs' \quad (9)$$

Now the air gap power Pg is given as:

$$Pg = \frac{\Pr cu}{S} = \frac{1}{S}(Vd.Id - S.rs.Id^2) \quad (10)$$

Since $Pg = Te.\omega_S$

$$Te.\omega_S = \frac{1}{S}(Vd.Id - S.rs.Id^2) \quad (11)$$

Now substituting from equation (5), the expression of electromagnetic torque is given as:

$$Te = \frac{(\frac{3\sqrt{6}}{\pi}\frac{VsL}{n1}Id - rs.Id^2)}{\omega_S} \quad (12)$$

The torque Te can be evaluated for known value of the dc link current using the above equation. Now, applying KVL in the dc equivalent circuit, the expression for the dc link current for the specified value of delay angle of the controlled converter is given as:

$$Id = \frac{3\sqrt{6}VsL}{\pi}(\frac{S}{n1} + \frac{Cos\alpha}{n2})/(Srs + 2Rr + Rd) \quad (13)$$

The expression for feedback power to the ac supply mains through the controlled converter is given as:

$$P_{fb} = -Vi.Id \quad (14)$$

The expression of output power Pm of the induction motor in terms of electromagnetic torque, number of poles, per unit slip and synchronous speed is given as:

$$Pm = Te\frac{2\omega(1-S)}{P} \quad (15)$$

The stator input power of the drive is the sum of output power and losses and is given as:

$$Pin = Pm + Ps + \Pr + Pdc + P_{fb} \quad (16)$$

The expression of stator copper loss is given as:

$$Ps = 2SRs'Id^2 \quad (17)$$

The expression of rotor copper loss is given as:

$$\Pr = 2Rr.Id^2 \quad (18)$$

The expression of power loss in dc link circuit is given as:

$$Pdc = Rd.Id^2 \quad (19)$$

The efficiency of the drive is given as:

$$\eta = \frac{Pm}{Pin}x100 \quad (20)$$

Using these performance equations, the steady state performance characteristics of the drive are computed using computer program based on the computer algorithm.

IV. COMPUTER ALGORITHM

The steady-state performance characteristics of static SER controlled slip ring induction motor drive are obtained using performance equations of the dc

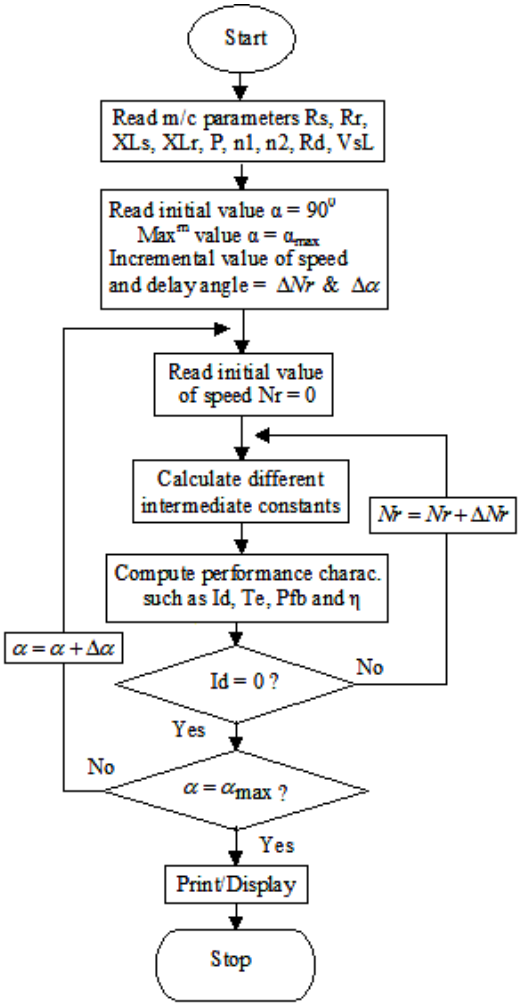

Fig. 5 Flow chart for computing Steady-state performance characteristics of the drive

equivalent circuit model. The Matlab software is used to solve mathematical equations. The flow chart of the computer algorithm is shown in Fig. 5. Initially, the values of parameters of the induction motor, recovery transformer, smoothing inductor and the supply voltage, such as, Rs, Rr, XLs, XLr, P, n1, n2, Rd and supply voltage VsL are supplied to the program. The value of these parameters are given in Appendix. The initial value of the delay angle α, incremental value of rotor speed ΔNr and incremental value of delay angle $\Delta\alpha$ are also supplied. ΔNr is increased in a step of 1 rpm and $\Delta\alpha$ in a step of 9^0. At particular value of the delay angle of the controlled converter, the different performance characteristics like dc link current Id, electromagnetic torque Te, power feedback to the ac supply mains Pfb and efficiency η of the drive system are computed at different speeds. These performance characteristics are also computed for other sets of the delay angles of the controlled converter by repeating of the computer program.

V. EXPERIMENTAL INVESTIGATION

The experimental setup of the drive is microprocessor based. The configuration of the control scheme is shown in Fig. 6. The synchronizing circuit generates three numbers of digitized signals which are in phase with line voltages applied to the thyristors of the controlled converter. These signals are applied to the microprocessor through pins PC0, PC1 and PC2 of port C_{lower} to provide information to the microprocessor about which one thyristor pair of the controlled converter is forward biased. The synchronizing circuit also generates three phase zero crossing signals which are applied to the microprocessor through interrupt pin RST 7.5. For the control of the delay angle, the system software which consists of one main program and two numbers of service subroutine programs, one for RST 7.5 and another for RST 6.5 is used. The main program initializes stack pointer, ports of intel-8255 and counters of 8253. It also controls interrupts and facilitates operation of RST 7.5 and RST 6.5 interrupt subroutines. After initialization the microprocessor waits for zero crossing signals through RST 7.5. First function of service subroutine RST 7.5 is to calculate address of the count value corresponding to the delay angle. The second function of the subroutine is to calculate the address of delay command word which indicates the pair of thyristors to be gated. After completion of this subroutine, the program returns to the main program where it waits for interruption through RST 6.5 at the terminal count of the count value. This subroutine provides firing pulses to the selected pair of thyristors and low level signals to the

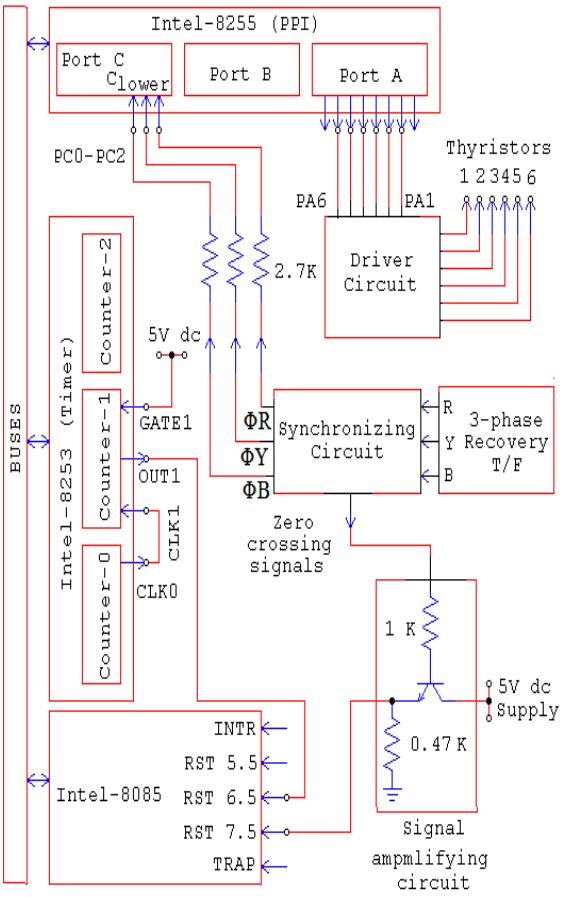

Fig. 6 Block diagram of microprocessor based control scheme of the drive

rest of the thyristors of the controlled converter for each pulse of zero crossing signals through pins PA1-PA6 of Port A. These firing pulses are amplified and shaped properly using driver circuits for proper firing of the thyristors.

VI. DISCUSSION OF RESULTS

The steady- state performance characteristics of static SER controlled slip ring induction motor drive are computed at the delay angles of 91^0, 100^0 and 109^0 of the controlled converter using dc equivalent circuit model. The computed results are compared with those of experimental ones to see the accuracy of the developed model. The performance characteristics are shown in figures Fig. 7. The figures of Fig. 7 (a) show the variation of torque with speed. The patterns of the characteristics indicate that the range of speed control of the drive decreases with increase in the delay angle. The figures of Fig. 7 (b) show the amount of power recovered to the ac supply mains as a function of speed of the drive. It is observed that the recovered power increases with the

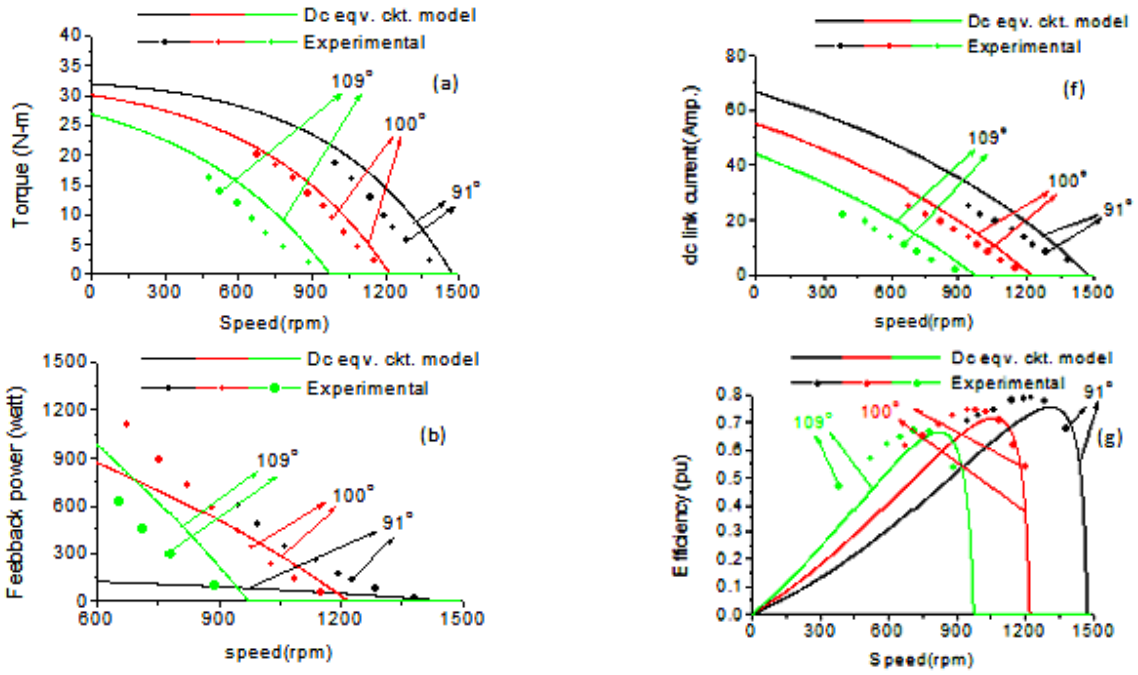

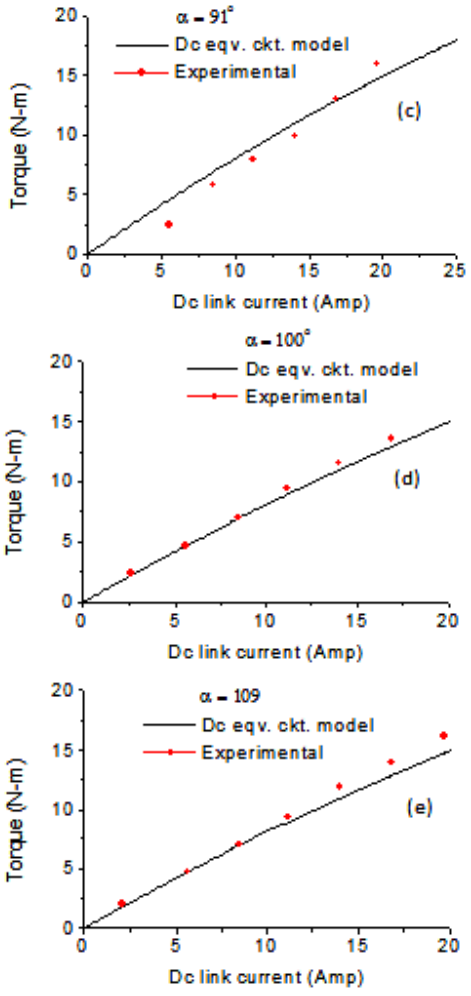

Fig. 7 Steady state performance characteristics of the drive at different values of the delay angle of the controlled converter ($\alpha = 91^0, 100^0, 109^0$) (a) Torque - speed (b) Feed back power - speed (c) Torque - dc link current at 91^0 (d) Torque - dc link current at 100^0 (e) Torque - dc link current at 109^0 (f) Dc link current – speed (g) Efficiency- speed

decrease of speed at fixed value of the delay angle. The figures from Fig. 7 (c) to Fig. 7 (e) represent the variation of the torque with the dc link current. It is observed that the torque of the drive varies linearly with the dc link current irrespective of the delay angle of the controlled converter. This exhibits that the drive has similar characteristics as that of separately excited dc motor in which torque varies linearly with the armature current. The variation of the dc link current with speed for different delay angles is shown in figure Fig. 7 (f). It is observed that by increasing the delay angle at constant value of the dc link current, the range of speed control of the drive is reduced. Fig. 7 (g) shows the pattern of efficiency with the variation of speed of the drive. It is evident from this figure that at a given value of the delay angle, the efficiency increases with the increase in speed almost in linear fashion and then, there is a steep decay in the narrow zone of speed. Also, the efficiency of the drive increases with the increase of the delay angle at a given value of speed in the lower range of speed but the peak of the efficiency is higher at lower value of the delay angle.

It is observed that the results predicted by dc equivalent circuit model fairly resemble with the

experimental results having deviation about twelve percent, whereas, the deviation predicted using synchronously rotating reference frame model is seventeen percent [7]. The attributed deviation is because of neglecting the effects of harmonics in rotor current, distortion in rotor current due to commutation overlap in the uncontrolled converter, ripple in dc link current and losses in semiconductor devices. The predicted performance characteristics using the proposed model is closer to the experimental ones in comparison to synchronously rotating reference frame model because the effect of voltage drop due to commutation overlap has been considered in the proposed model, whereas, it is neglected in synchronously rotating reference frame model

VII. CONCLUSIONS

In this paper steady state model of static SER controlled slip ring induction motor drive using dc equivalent circuit has been developed. The various performance characteristics have been predicted. The following conclusions are made from the study:

1. The torque of the drive varies linearly with the dc link current irrespective of the delay angle of the controlled converter. Hence, the drive has similar characteristics as of separately excited dc motor.
2. Keeping constant value of dc link current if the delay angle is increased, the speed decreases.
3. For a set value of the delay angle, the efficiency increases with the rise in speed.
4. The dc equivalent circuit model is simpler and can be used for predicting the performance of the drive with more accuracy in comparison to SRRF model.

REFERENCES

[1] Lavi, A. and Polge, R.J., "Induction motor speed control with static inverter in the rotor," IEEE Tran. on power apparatus and systems, vol PAS-85, no.1, Jan 1966, pp.76-84.

[2] Weiss, H. W., "Adjustable speed ac drives systems for pump and compressor applications," IEEE Tran. on Industry applications, vol. IA-10, no. 1, Jan/Feb 1974, pp 162-167.

[3] Olivier, G., Stefanovic, V.R. and April, G.E., "Evaluation of phase-commutated converters for slip-power control in induction drives," IEEE Tran. on industry applications, vol. IA-19, no. 1, Jan/Feb 1983, pp. 105-112.

[4] Pavlov, V., Okitsu, B., Suzuki, T., and Ohnishi, T., "Hybrid speed control system of wound rotor induction motor," Proc. IEE, Vol. 126, no. 9, 1979, pp. 821-825.

[5] Mittle, V. N., Venkatesan, K. and Gupta, S.C., "Switching transients in static slip energy recovery drive," IEEE Tran. on power apparatus and systems, vol. PAS-98, no. 4, July/Aug. 1979, pp. 1315-1320.

[6] Brown, J. E., Drury, W., Jones B. L., and Vas, P., "Analysis of the periodic transient state of a static Kramer drive," Proc. IEE, vol. 133, pt. B, no. 1, Jan. 1986, pp. 21-30

[7] Krause, P. C., Wasynczuk, O., and Hildebrandt, M. S., "Reference frame analysis of a slip energy recovery system," IEEE Tran. on energy conversion, vol. 3, no.2, June 1988, pp. 404-408.

[8] Akpinar, E. and Pillay, P., "Modeling and performance of slip energy recovery induction motor drives," IEEE Tran. on energy conversion, vol. 5, no. 1, March 1990, pp. 203-210.

[9] Papathanassiou, S. A. and Papadopoulos, M. P., "State space modeling and eigen value analysis of the slip energy recovery drive," Proc. IEE, Electric power application, vol. 144, no.1, Jan. 1997, pp. 27-36.

[10] Sen, P.C. and Ma, K.H.J., "Rotor chopper control for induction motor drive: TRC strategy, " IEEE Tran. on Industry applications, vol. IA-11, no.1, Jan./Feb. 1975, pp. 43- 49.

[11] Dubey, G.K., "Power semiconductor controlled drives," PHI. Edition.

APPENDIX

Slip ring induction motor: 3-phase, 5 hp, 400 volt, 7.5 amps, 50 Hz, 1440 rpm, Δ-Y connected

Parameters: Stator resistance = 5.386 Ω ; Rotor resistance = 0.446 Ω ; Stator leakage reactance = 14.311 Ω ; Rotor leakage reactance = 0.341 Ω ;Magnetizing reactance =193 Ω ; Stator to rotor turn ratio = 6.48 ;

Separately excited dc generator coupled with the motor: 5 hp, 220 volt, 17 amps, 1440 rpm

Parameters: Armature resistance = 2.436 Ω ; Generator constant = 1.42 volt/rad/sec.

Other Parameters of drive system: Turn ratio of recovery transformer = 6.0 ; Resistance of smoothing inductor = 0.2 Ω ; Inductor of smoothing inductor = 0.374 H